FUSION OF IMAGING SPECTROMETER AND LIDAR DATA USING SUPPORT VECTOR MACHINES FOR LAND COVER CLASSIFICATION IN THE CONTEXT OF FOREST FIRE MANAGEMENT

B. Koetz[a,*], F. Morsdorf[a], T. Curt[b], S. van der Linden[c], L. Borgniet[b], D. Odermatt[a], S. Alleaume[b], C. Lampin[b], M. Jappiot[b] and B. Allgöwer[d]

[a] Remote Sensing Laboratories (RSL), Dept. of Geography, University of Zurich, Winterthurerstrasse 190, CH-8057 Zurich, Switzerland, Email: bkoetz@geo.unizh.ch
[b] Cemagref, Aix-en-Provence, Mediterranean ecosystems and associated risks research unit, 3275 route de Cézanne-CS 40061-13182 Aix en Provence cedex 5, France
[c] Geomatics Department, Humboldt-Universität zu Berlin, Unter den Linden 6, D-10099 Berlin, Germany
[d] Geographic Information Systems, Dept. of Geography, University of Zurich, Winterthurerstrasse 190, CH-8057 Zurich, Switzerland

Commission VII, WG 1

KEY WORDS: Support Vector Machines, land cover classification, hyperspectral, LiDAR, multi-sensor fusion

ABSTRACT:
A combination of the two remote sensing systems, imaging spectrometry (IS) and Light Detection And Ranging (LiDAR), is well suited to map fuel types, especially within the complex wildland urban interface. LiDAR observations sample the spatial information dimension describing geometric surface properties. Imaging spectrometry on the other hand samples the spectral dimension, which is sensitive for discrimination of species and surface types. As a non-parametric classifier Support Vector Machines (SVM) are particularly well adapted to classify data of high dimensionality and from multiple-sources as proposed in this work. The presented approach achieves an improved land cover mapping based on a single SVM classifier combining the spectral and spatial information dimensions provided by imaging spectrometry and LiDAR.

1. INTRODUCTION

Accurate description of wildland fuel types and fuel properties is vital for understanding the processes involved in initiation and propagation of forest fires (Carlson and Burgan 2003). Remote sensing offers the potential to provide spatially distributed information on fuel types important for the assessment of fire risk and to mitigate the impact of wildland fires (Chuvieco 2003; Justice et al. 2003). Data of the two remote sensing systems, imaging spectrometry and LiDAR, are well suited to map the diverse and heterogeneous fuel types, especially within the complex Mediterranean environment and the wildland urban interface (WUI).
Land cover monitoring in the context of forest fire management enables the assessment of the spatial distribution for different fuel types. The classification of fuel types is specifically dependant on the height, density and the surface type of the fuel. LiDAR observations sample the spatial information dimension describing the geometric properties of natural and artificial surfaces (Andersen et al. 2005; Morsdorf et al. 2004). Imaging spectrometry on the other hand samples the spectral dimension, which is sensitive for discrimination of species, surface types and fuel moisture (Jia et al. 2006; Kötz et al. 2004). The observations of these two remote sensing systems can mutually complement each other and are thus indispensable for comprehensive and specific fuel type mapping. Spatial distribution of land cover together with additional properties on the fuel structure and condition can be further translated into fuel models important for the parameterization of forest fire behaviour models.
The synergistic use of LiDAR and spectral data has already been exploited for land cover mapping purposes (Hill and Thomson 2005; Hodgson et al. 2003; Packalen and Maltamo 2007). Nevertheless commonly used statistical classification methods, such as maximum likelihood classification, are limited to classify high dimensional data typically provided by multiple sources (Benediktsson et al. 1990). With increasing numbers of input dimensions and complexity of the data the description of an appropriate multivariate model required by statistical approaches becomes unpractical. Several non-parametric classifiers have been introduced which do not require such prior knowledge on the statistical distribution of the data to be classified.
Being such a non-parametric classifier Support Vector Machines (SVM) are particularly well suited to classify data of high dimensionality and from multiple sources (Waske and Benediktsson 2007 (in review)). SVM delineate two classes by fitting an optimal separating hyperplane to those training samples that describe the edges of the class distribution. As a consequence they generalize well, even when only small training sets are available for the classification of high dimensional data (Pal and Mather 2006).
Within the presented study we focus on mapping fuel types at landscape level based on airborne LiDAR and imaging spectrometer data over a Mediterranean site south of Aix-en-Provence.
The final performance of the data fusion approach is assessed by the accuracy of the classification based on the combined imaging spectrometry and LiDAR data compared to a pure spectral classification input.

2. DATA

An airborne survey was conducted early October 2006 over a Mediterranean site south of Aix-en-Provence, France. The covered site comprised typical Mediterranean vegetation intermixed with urban structures. Vegetation covered a typical range of French Mediterreanean wildland fuels: (i) fire-resistant matorrals (so-called garrigue) dominated by species such as the sclerophyllous *Quercus coccifera* and *Ulex* spp.; (ii) fire-prone *Pinus halepensis* woodlands; and (iii) fire-resistant *Quercus* woodlands (*Q. ilex*, *Q. pubescens*). These three predominant vegetation types are mixed as a function of fire history and vegetation dynamics (Quézel and Médail 2003). These vegetation types are intermingled with human settlements and buildings forming a wildland-urban interface. This entails frequent management practices of vegetation in the region such as shrub-clearing of the understorey, and thinning of the overstorey.

The employed remote sensing systems the LiDAR (Optech, ALTM3100) and the imaging spectrometer (AISA-Eagle) were mounted together with a very high-resolution photogrammetric camera (40 cm spatial resolution) on a helicopter and operated by the company HELIOGS. The airborne survey was organized to cover a region of about 13.6 x 3.6 km in a spatial resolution of 1 meter. In the presented study only subset is presented (Fig. 1-2).

After pre-processing, LiDAR derivatives and spectral bands of the imaging spectrometer were co-registered and as layer stack jointly considered for the classification. Parallel to the airborne survey a comprehensive field campaign was conducted for the validation of the fuel types derived from the observations of the two remote sensing systems. The field measurements collected describe the relevant fuel types, including a specific characterization of the WUI interface and species composition. Fuel properties such as biomass and fuel moisture content were also sampled.

2.1 Imaging Spectrometer

The imaging spectrometer data employed in this study has been recorded by the AISA/Eagle imaging spectrometer (Tab. 1). The proposed thematic analysis required a dedicated geometric and radiometric pre-processing of the imaging spectrometer data. The image data was geometrically corrected by the parametric geocoding approach PARGE. Topography and illumination effects were taken into account based on the digital surface model provided by the LiDAR. Remaining geometric inaccuracies caused by erroneous synchronization with the inertial navigation system had to be corrected by a direct co-registration to the LiDAR data. Subsequently the physically based atmospheric correction software ATCOR4 was employed to obtain top-of-canopy reflectance (Richter and Schläpfer 2002; Schläpfer and Richter 2002) (Fig. 1). The original spectral range and resolution have been reduced due to data quality issues to 454-923 nm and 4.6 nm respectively.

Image area	Ground resolution	Spectral bands
2000 x 370m FOV: 36.7°	1 m IFOV: 0.036°	244 bands with 2.3 nm width 400-970 nm

Table 1. Specifications of the AISA/Eagle imaging spectrometer data

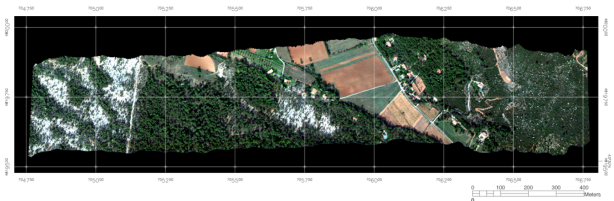

Figure 1. Geometrically and radiometrically corrected AISA/Eagle data of the study site (true colour composite)

2.2 LiDAR

The LiDAR system used was the Airborne Laser Terrain Mapper ALTM3100 laser scanner developed by the Canadian company Optech (Tab. 2). The ALTM3100 system is a laser rangefinder recording up to four returns of the laser signal from the ground surface. For a small subset of 2 x 1.5 km the full waveform of the laser return signal was also recorded with the Optech waveform digitizer. The survey was conducted with a nominal height above ground of 1000 m. This leads to average point density of 3.7 points per square meter (p/m^2) enabling the processing of elevation models of the surface and terrain in the spatial resolution of one meter (Fig. 2).

Several simple derivatives describing the vertical and horizontal geometric surface properties are retrieved from the original LIDAR return distribution similar to (Naesset 2002; Naesset and Gobakken 2005). The vertical height distribution of laser returns within gridded 3 x 3 meter boxes was described by six height percentiles. Furthermore point density for six equidistant layers was derived based on the same vertical return distribution for an assessment of the vertical density distribution. Finally the difference between the digital surface and the terrain model provided an estimate of the canopy height model, which also included heights of artificial structures. All LiDAR derivatives were normalized to their respective maximal values facilitating the optimization of the SVM classification parameters.

Scan angle	Ground resolution	Point density	Laser wavelength
FOV: ±25°	1 m pixel size (DTM & DSM)	3.7 points/m^2	1064 nm

Table 2. Specifications of the ALTM3100 LiDAR (Optech)

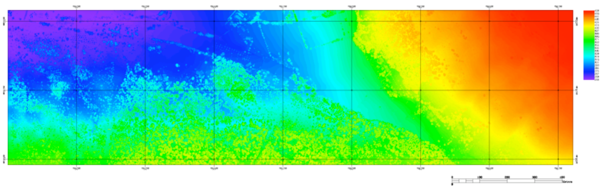

Figure 2. Digital surface model (DSM) obtained by the Optech laser scanner ALTM3100 of the study site

3. METHODS

The land cover classification was performed by the non-parametric Support Vector Machines (SVM). The SVM classification was trained and applied to three different data sets representing different input sources and information dimensionality (Fig. 3).

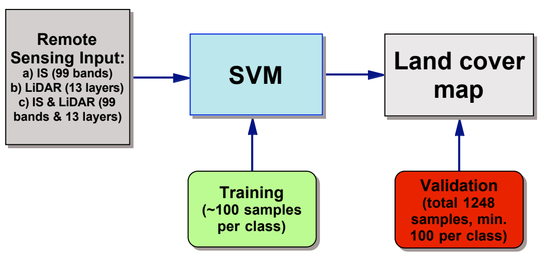

Figure 3. Processing flow of SVM classification setups a-b) single sources and c) multiple remote sensing sources

3.1 Support Vector Machines

SVM split two classes by constructing an optimal separating hyperplane, which maximizes the distance between the two classes (Fig. 4) (Burges 1998). This hyperplane is fitted only to the training samples that describe the margins of the corresponding classes. For linear non-separable cases the data is mapped into a higher dimensional feature space that allows a linear hyperplane to split the classes newly distributed data.

Separate SVM were trained for different remote sensing inputs (Fig. 3): single sources: Imaging spectrometer (IS, 99 bands), LiDAR (13 layers) and as multiple source: IS and LiDAR combined in a layer stack (99 bands + 13 layers).

To solve the multi-class problem with the originally binary SVM a one-against-all (OAA) strategy was applied (Foody and Mathur 2004): a set of binary classifiers is trained to individually separate each class from the rest. The final class label is then determined by selecting the maximum decision value, i.e. the distance of a pixel to the separating hyperplane, from the set of OAA outputs.

The training of the SVM was performed using the ν-SVM approach in LIBSVM (Chen and Lin 2001). A Gaussian kernel was used to transform the data (Vapnik 1998). In this case, two parameters needed to be set for the training: the parameter γ that controls the width of the Gaussian kernel and ν, an upper bound on the fraction of training errors and a lower bound of the fraction of support vectors (Schoelkopf et al. 2000). The more common C-SVM and the applied ν-SVM lead to similar results, but ν-SVM were chosen as they require less processing time. An IDL-implementation of LIBSVM for remote sensing data was used to train wide ranges of values for γ [0.001-1000] and ν [0.001-0.2]. Subsequently the quality of the resulting classification was evaluated based on a 16-fold cross validation (Janz et al. 2007). This way, optimal parameters could be found for each binary OAA classifier and an overfitting to the reference data was avoided.

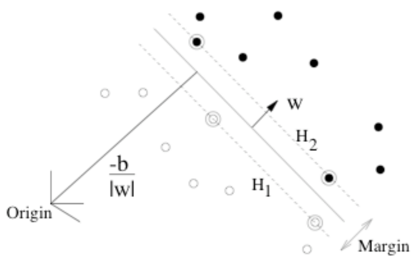

Figure 4. Fitting of a hyperplane (Burges 1998)

3.2 Classification: training and validation

A classification scheme specifically adapted to the characteristics of the wildland urban interface was developed based on the fuel type classification of the European PROMETHEUS project and the experiences in mapping urban areas (Herold et al. 2003). The classification scheme is divided into different levels as presented in Table 3. The first and second level represent functional categories and land cover classes relevant for fuel type discrimination. The third level is thematically divided by surface properties and could be extended to include different vegetation functional types or species. Only classes present in the covered area could be considered amounting up to a number of nine land cover classes.

The accuracy of a supervised classification depends significantly on the training data set. Specifically for training of SVM it is important to include mixed pixels at the border of class boundaries, as they are most efficient to determine the hyperplane between two classes (Foody and Mathur 2006). Therefore, a clustered sampling strategy was performed. For each class seed points were randomly selected where a 5 x 5 pixel cross was sampled similar to (van der Linden et al. submitted). This strategy helped to cover the class internal heterogeneity of the different classes as well as to include mixed pixels along with adjacent pure pixels to describe the position of the hyperplane. The samples were labeled based on very high-resolution aerial photographs acquired along with the remote sensing data. For discrimination of vertical properties for certain classes, such as shrubs, the canopy height model was consulted. For each class about 100 samples were selected. For classes with a low areal coverage, such as swimming pools and roofs, a lower number of samples had to be taken.

For the accuracy assessment of the different classification results an independent validation set was collected by unstratified randomized sampling (900 samples). Additional stratified randomized sampling was necessary for underrepresented classes (roof tiles, swimming pool, road asphalt, road gravel, bare soil, bare rock) adding up to 100 samples for each class. A total of independent 1248 samples were selected and labeled to one of the land cover classes based on the very high-resolution aerial photographs.

Level 1	Level 2	Level 3
Built up	Buildings/roof	Wood shingle roof
		Tile roof
		Metal roof
		Concrete roof
	Transportation areas	Asphalt road
		Concrete road
		Gravel road
		Parking lot
	Sport infrastructure	Tartan court
Vegetation	Ground fuels (< 30 cm)	Grass & agricultural fields
	Shrub / Garriuges (< 2 m)	* extendable for different vertical structure & species
	Tree stands	* extendable for different vertical structure & species
Non-urban bare surfaces	Bare soil	
	Bare rock	
Water bodies	Swimming pools	
	Natural water bodies	

Table 3. Landcover classification scheme adapted for fuel type mapping in the wildland urban interface

4. RESULTS AND DISCUSSION

The performance of the different SVM classifications were assessed using confusion matrices and user's accuracy (Congalton and Green 1999). Three SVM classifications based on different remote sensing inputs have been validated separately to assess the advantages for land cover mapping of each sensor system and the improvement of the multiple-source fusion.

The SVM classification of the imaging spectrometer data provided acceptable results in terms of overall accuracy and kappa coefficient (Tab. 4). Class specific results reveal significant classification confusion between spectrally similar classes such as the three vegetation classes, which lead to moderate user accuracies (Fig. 5). Also some confusion between bare rock and ground fuel is evident caused probably by mixed pixels.

The overall classification performance of the pure LiDAR data was poor, but nevertheless provided significant user accuracies for classes with properties in the vertical dimension (Fig. 5).

Especially the class roof tiles performed very well, which probably can probably be explained by the absolute height above ground with concurrent opaqueness of roofs as opposed to tree canopies, which are semi-transparent three-dimensional objects. The moderate results for the shrub class is caused by issues with the vertical separability of laser returns for low canopies. Further for shrubs with high canopy density the laser is incapable of penetrating to the ground. Both issues lead to the lack of the vertical information content in the LiDAR data for certain shrub canopies.

The joint classification of the multiple sources, imaging spectrometer and LiDAR, leads to a significant improvement in terms of overall accuracy and kappa (Tab. 4). The inclusion of classes with similar geometric but different spectral properties, such as roofs of different materials (e.g. in Tab. 3), would even increase this improvement. Most of the achieved improvement in accuracy for the multiple-source classification can be explained by the decreased confusion between the vegetation classes. The vertical information content of the LiDAR observations was especially helpful to separate the classes ground fuel and tree canopy. LiDAR provides relatively to spectral information content no additional information on the class shrub due to the issues related to vertical separability of laser returns and vegetation density. Further, spectrally similar classes such as bare soil and roof tiles made of similar material could better be separated by the vertical information provided the LiDAR. This effect was not revealed by the confusion matrix but is visible in the land cover maps (Fig. 6).

Remote sensing input	Overall Accuracy	Kappa coefficient
IS & LiDAR	75.4 %	0.716
IS	69.15 %	0.645
LiDAR	31.73 %	0.226

Table 4. Accuracy assessment of the SVM classifications

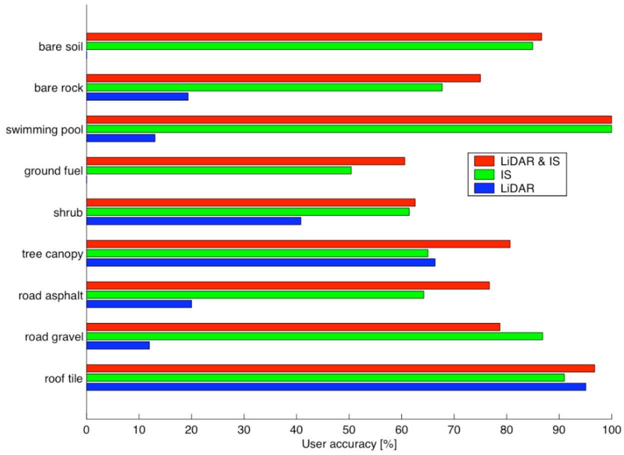

Figure 5. User accuracy of SVM classification performances based on different remote sensing data input

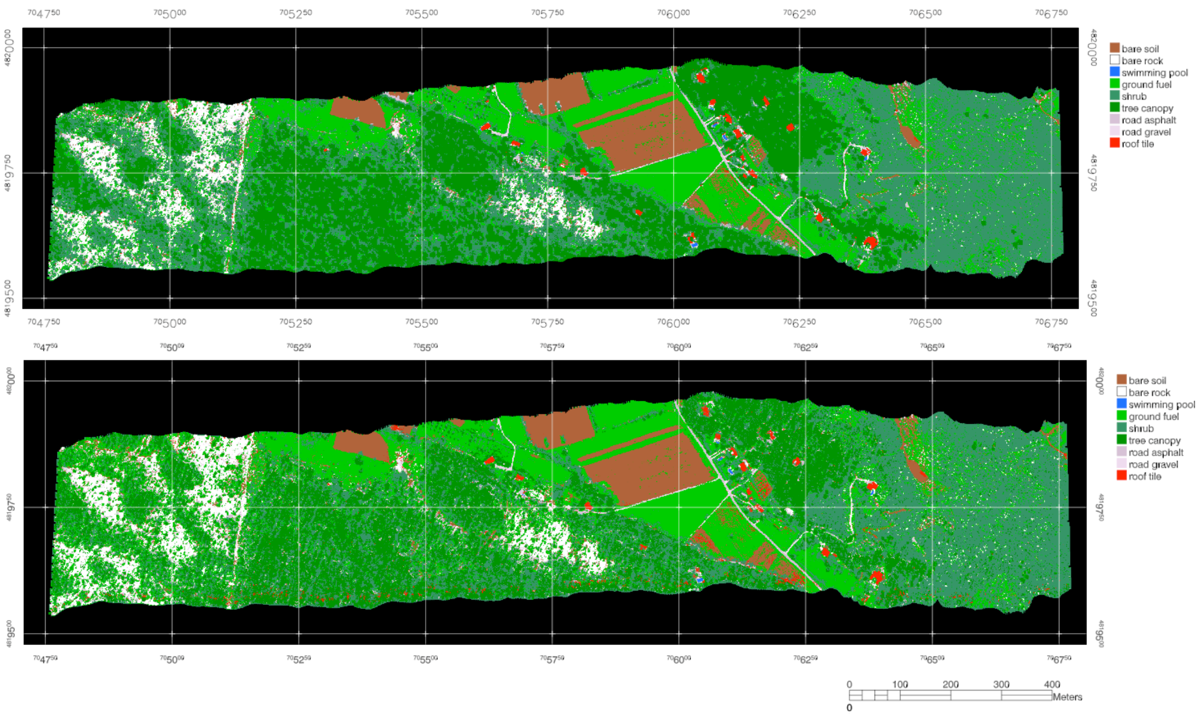

Figure 6. Land cover maps based on the different SVM classifications, upper map: product based on the multiple input sources IS & LiDAR, lower map: product based on the single input source IS

5. CONCLUSIONS

The Earth observation requirements within several scientific fields, such as urbanization, biodiversity and natural hazards, demand land cover monitoring of landscapes with increasing complexity and in ever higher levels of detail. The commonly used approach of land cover classification based on multi-spectral data is limited by the spectral similarity of certain surface types. Further, three-dimensional features of important surface types, such as built-up urban construction or vertical vegetation structure, are not directly inferable from the spectral information content provided by passive optical sensors. Due to this underdetermined and partly indirect relationship, the interpretation of remote sensing data for land cover monitoring should rely on as many independent observations as possible. This conclusion leads to the combined exploitation of multiple information sources as provided for example by complementary sensor systems. The increased dimension and complexity of such information also requires new classification methods to adequately interpret the data of multiple information sources.

The method presented in this study is capable of a joint one-step SVM classification for the fusion of multiple-source remote sensing data provided by an imaging spectrometer and a LiDAR. The SVM classifier was able to efficiently exploit the significantly increased information content in the (hyper)spectral and the three-dimensional dimension. Specifically the SVM generalized well, even when only small training sets were available for the classification of the high dimensional data provided the multiple data sources. The three-dimensional information of the LiDAR data complemented well the spectral information leading to a significant increase in the overall land cover classification accuracy relative to the pure spectral information input. Important features of fuel types as the vertical structure vegetation and houses could be assessed with higher accuracy and reliability. This enhanced mapping of the wild land urban interface can be a significant input to forest fire behaviour models leading to improved risk assessment and mitigation of forest fires.

ACKNOWLEDGEMENTS

This study has been funded by the EC integrated project FIRE PARADOX. The employed SVM classification tool has been developed by Andreas Janz (Humboldt-Universität) whose support is very much appreciated. The airborne survey of the imaging spectrometer and the LiDAR has been conducted by the HELIOGS.

REFERENCES

Andersen, H.E., McGaughey, R.J., & Reutebuch, S.E. (2005). Estimating forest canopy fuel parameters using LIDAR data. *Remote Sensing of Environment, 94*, 441-449

Benediktsson, J.a., Swain, P.H., & Ersoy, O.K. (1990). Neural Network Approaches Versus Statistical-Methods in Classification of Multisource Remote-Sensing Data. *Ieee Transactions on Geoscience and Remote Sensing, 28*, 540-552

Burges, C.J.C. (1998). A Tutorial on Support Vector Machines for Pattern Recognition. *Data Mining and Knowledge Discovery, 2*, 121-167

Carlson, J.D., & Burgan, R.E. (2003). Review of users' needs in operational fire danger estimation: the Oklahoma example. *International Journal of Remote Sensing, 24*, 1601-1620

Chen, C.-C., & Lin, C.-J. (2001). LIBSVM: a library for support vector machines. In: http://www.csie.ntu.edu.tw/~cjin/libsvm

Chuvieco, E. (Ed.) (2003). *Wildland Fire Danger Estimation and Mapping: The Role of Remote Sensing Data*. Singapore: World Scientific

Congalton, R.G., & Green, K. (1999). *Assessing the Accuracy of Remotels Sensed Data: Principles and Practices*. Boca Raton: Lewis

Foody, G.M., & Mathur, a. (2004). A relative evaluation of multiclass image classification by support vector machines. *Ieee Transactions on Geoscience and Remote Sensing, 42*, 1335-1343

Foody, G.M., & Mathur, a. (2006). The use of small training sets containing mixed pixels for accurate hard image classification: Training on mixed spectral responses for classification by a SVM. *Remote Sensing of Environment, 103*, 179-189

Herold, M., Gardner, M.E., & Roberts, D.A. (2003). Spectral resolution requirements for mapping urban areas. *Ieee Transactions on Geoscience and Remote Sensing, 41*, 1907-1919

Hill, R.A., & Thomson, A.G. (2005). Mapping woodland species composition and structure using airborne spectral and LiDAR data. *International Journal of Remote Sensing, 26*, 3763-3779

Hodgson, M.E., Jensen, J.R., Tullis, J.A., Riordan, K.D., & Archer, C.M. (2003). Synergistic use of lidar and color aerial photography for mapping urban parcel imperviousness. *Photogrammetric Engineering and Remote Sensing, 69*, 973-980

Janz, A., Schiefer, S., Waske, B., & Hostert, P. (2007). A user-oriented tool for advanced classification of hyperspectral data using support vector machines. In, *EARSeL Imaging Spectroscopy workshop*. Bruegge

Jia, G.J., Burke, I.C., Goetz, A.F.H., Kaufmann, M.R., & Kindel, B.C. (2006). Assessing spatial patterns of forest fuel using AVIRIS data. *Remote Sensing of Environment, 102*, 318-327

Justice, C.O., Smith, R., Gill, A.M., & Csiszar, I. (2003). A review of current space-based fire monitoring in Australia and the GOFC/GOLD program for international coordination. *International Journal of Wildland Fire, 12*, 247-258

Kötz, B., Schaepman, M., Morsdorf, F., Bowyer, P., Itten, K., & Allgower, B. (2004). Radiative transfer modeling within a heterogeneous canopy for estimation of forest fire fuel properties. *Remote Sensing of Environment, 92*, 332-344

Morsdorf, F., Meier, E., Kötz, B., Itten, K.I., Dobbertin, M., & Allgower, B. (2004). LIDAR-based geometric reconstruction of boreal type forest stands at single tree level for forest and wildland fire management. *Remote Sensing of Environment, 92*, 353-362

Naesset, E. (2002). Predicting forest stand characteristics with airborne scanning laser using a practical two-stage procedure and field data. *Remote Sensing of Environment, 80*, 88-99

Naesset, E., & Gobakken, T. (2005). Estimating forest growth using canopy metrics derived from airborne laser scanner data. *Remote Sensing of Environment, 96*, 453-465

Packalen, P., & Maltamo, M. (2007). Th k-MSN method for the prediction of species-specific stand attributes using airborne laser scanning and aerial photographs. *Remote Sensing of Environment, in press*

Pal, M., & Mather, P.M. (2006). Some issues in the classification of DAIS hyperspectral data. *International Journal of Remote Sensing, 27*, 2895-2916

Quézel, P., & Médail, F. (2003). *Ecologie et biogeography des forêts du basin méditerranéeen*. Paris: Elsevier

Richter, R., & Schläpfer, D. (2002). Geo-atmospheric processing of airborne imaging spectrometry data. Part 2: atmospheric/topographic correction. *International Journal of Remote Sensing, 23*, 2631-2649

Schläpfer, D., & Richter, R. (2002). Geo-atmospheric processing of airborne imaging spectrometry data. Part 1: parametric orthorectification. *International Journal of Remote Sensing, 23*, 2609-2630

Schoelkopf, B., Smola, A., Williamson, R., & Bartlett, P.L. (2000). New support vector algorithms. *Neural Computation, 12*, 1207-1245

van der Linden, S., Janz, A., Eiden, M., & Hostert, P. (submitted). Classifying segemented hyperspectral data from urban areas using support vector machines. *Journal of Applied Remote Sensing*

Vapnik, V.N. (1998). *Statistical Learning Theory*. New York: Wiley

Waske, B., & Benediktsson, J.A. (2007 (in review)). Fusion of Support Vector Machines for Classification of Multisensor Data. *Ieee Transactions on Geoscience and Remote Sensing*